PHYSICAL REVIEW A VOLUME 48, NUMBER 2 AUGUST 1993

Wave mechanics of particle detectors

A. A. Broyles
Department of Physics, Institute for Fundamental Theory, University of Florida, Gainesville, Florida 32611
(Received 11 December 1992)

The operations of many detection devices are usually explained in terms of the ionization tracks produced by classical charged particles. A wave-mechanical analysis does not seem to be available. Mott [Proc. R. Soc. London Ser. A **126**, 79 (1929)] has shown that an incident α wave emitted by a radioactive nucleus would be scattered by atoms primarily in directions almost forward. However, these scattered waves would appear over the entire sensitive region of the detector. The mechanism that produces a collapse of the wave function to a single track is analyzed here. The incident α wave is written as a superposition of minimum-sized packets. Since it is linear, the Schrödinger equation for the system including an observer can be solved for each packet individually. After the minimum packets interact with the electrons in the detector, they cannot be recombined to form a plane wave. However, they can be combined in groups to form larger coherent packets interacting with the detector to form tracks. The size and shape of each coherent packet are determined by the properties of the medium that is ionized to produce its track. The track from each packet is seen by the observer and is associated with a state of his memory, recording only one track. Each such packet replaces the particle in the usual explanation. These are the packets required to predict the quantum jumps seen in the scattering of laser light from an isolated atom as I have discussed [Phys. Rev. A **45**, 4925 (1992)]. The relation of the probability distribution of these tracks to the wave function is explained.

PACS number(s): 03.65.Bz, 06.70.Dn, 29.40.Cs, 29.40.Gx

I. INTRODUCTION

The operation of a detection device such as a cloud chamber, Geiger counter, bubble chamber, drift chamber, or photographic plate is often explained in terms of an incident classical particle that produces a wake of ionized atoms in a sensitive medium. On this wake is formed droplets, bubbles, or exposed grains that are visible to the naked eye in a cloud chamber, bubble chamber, or photographic plate. On the other hand, quantum mechanics usually calls for an incident wave function extending over the entire sensitive region of the detector. Mott [1] has shown that this incident wave will scatter off of the atoms largely in almost forward directions. However, since the scattering atoms are present in the entire volume, these scattered waves will cover the entire sensitive volume of the detector. The questions still remain how a wave function with a broad extent collapses to a track, and what causes the probability distribution of observed tracks to be proportional to the magnitude squared of the incident wave.

Some physicists [2] have cited this success of classical-particle theory and the lack of a wave-mechanical explanation as evidence for a dual wave-particle nature of the elementary constituents of quantum mechanics. This kind of ambiguity at the foundations increases the difficulty of teaching quantum mechanics and leaves students with the feeling that physics is based on imprecise concepts. In addition it causes many physicists to have doubts about when to use the particle approach and when to think of a wave in their research. We shall see here how a uniform incident wave can result in a single, well defined, ionization track thus removing this argument for the introduction of the particle concept into quantum mechanics. Since no use will be made of particles, we shall refer to α waves rather than to α "particles."

A previous paper [3] has presented an explanation of the jumps in the observed intensity of laser light scattered off of a trapped isolated atom. That analysis assumed that a detector would associate each recorded state with a packet of the laser light. The manner in which a detector produces this association is discussed in Sec. V.

In Fig. 1 is shown the tracks produced by the α waves (of roughly 5 MeV energy) from radioactive decays at the center of a cloud chamber. Although each α wave produces a single track, the fact that these tracks can be clearly seen shows that visible light passes through the medium coherently. This means that, after a portion of the visible light has passed out of the cloud chamber, the atoms that were excited to produce the scattered wave have returned to their original state. As a consequence, the wave function for the cloud chamber plus these light waves can be written as a product of this initial cloud-chamber state multiplied by the light wave amplitudes at times both *before* and *after* the scattering. See Heitler's book [4]. This is obviously not the case for α waves since the final state of the cloud chamber has the ions and droplets that make up the track while the initial state does not.

In Sec. II, we consider, as a specific example, the detection of an α wave from a radioactive nucleus in a cloud chamber. This wave is emitted in a single transition of a nucleus. The analysis of this emission in terms of the leakage of an α wave through a nuclear barrier was made

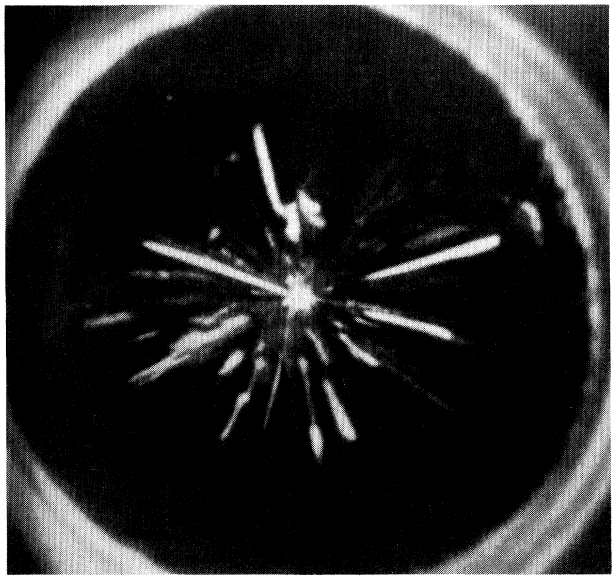

FIG. 1. Photograph of α tracks in a cloud chamber from a radioactive source in the center. The tracks do not cover the sensitive area of the cloud chamber although the wave function does. This is Fig. 41-44 from *Physics Demonstration Experiments*, edited by H. F. Meiners, ©1970 by the American Association of Physics Teachers. Reprinted by permission of John Wiley & Sons, Inc.

by Gamow and by Gurney and Condon [5] (see Fig. 2), but we shall be concerned only with the fact that such a wave interacts with a cloud chamber. To simplify the discussion, we shall take a rectangular cloud chamber with an essentially plane α wave incident normal to one of the surfaces as shown in Fig. 3. The walls of the chamber will be assumed to be completely transparent.

A cloud chamber involves many atoms so that the exact solution of the Schrödinger equation for such a system would be prohibitively complicated. However, a sufficient understanding of the form of this solution to reveal how an incident α wave produces a single track can be obtained by means of the analysis presented in this paper. The techniques used will be similar to those developed by von Neumann [6,7] for his measurement theory. We

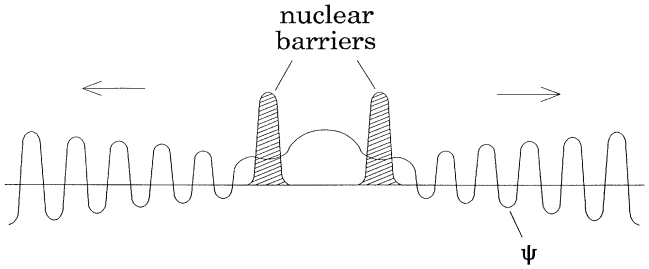

FIG. 2. The wave function for an α "particle" leaks through the nuclear barriers according to the analysis of Gamow and Gurney and Condon.

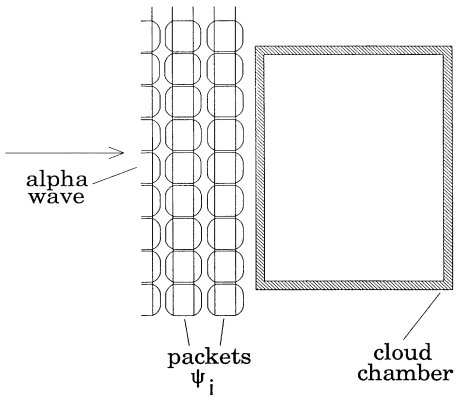

FIG. 3. The α wave is approximately plane and propagates normal to one face of the cloud chamber. This wave can be written as a superposition of packets ψ_i.

shall add another simplification to these considerations by restricting ourselves to α waves with energies equal to or greater than 5 meV. This allows us to approach the problem in a manner similar to that used by Bohr [8] in his consideration of the stopping power of materials for heavy particles.

The approach used here to determine the wave function of the α wave and the detector is to first write the α wave as a superposition of packets of the minimum size that allows them to remain small as they move in the cloud chamber. Since the Schrödinger equation is linear, the wave function for the α wave plus the detector can be found for each of these packets, and then these components can be recombined to form the entire wave function. Before they enter the cloud chamber, these packets can be recombined into the incident plane wave multiplying the wave function for the detector. After they enter the sensitive medium, however, each packet interacts with the medium to form a track that is finally seen as tiny droplets. Since the tracks for different minimum packets involve different excitations of the medium, they cannot be recombined into a plane wave. However, each portion of the wave function representing a track can be written as the sum of a term proportional to the wave function of a particular selected track and a remainder. Those components proportional to a single track wave function can be combined so that their minimum α packets add to form a larger coherent packet. The wave function after the interaction can take the form of a superposition of these larger coherent packets with their wakes. Since their wakes are different, these larger packets cannot be combined after they have entered the medium. Their dimensions are determined by the properties of the medium.

To understand why an observer sees only one track, in Sec. III we consider a system that includes, not only the α wave and the cloud chamber, but also the observer. Since the wave function is linear, its form can be determined, as before, by solving the Schrödinger equation for each coherent packet at a time and then summing over these solutions. The solution for each such packet will result in

an observer state with the memory of only one track. As noted in the last paragraph, the terms of the wave function constructed from different coherent packets cannot be combined. As a result, the final wave function takes the form of the sum of these terms, each term involving one coherent packet and an observer state with the memory of only one track.

A very similar analysis can be applied to any detector whose operation involves an ionized track. For example, a scintillation screen, such as that used by Rutherford [9] to detect α waves or like that at the end of a cathode ray tube that responds to electrons, produces ionized regions that emit visible light. Photographic plates exhibit tracks of exposed grains. These ionized regions are produced by the Coulomb fields of coherent packets formed in the same way as we have described for an α wave in a cloud chamber. We consider in Sec. IV the answer to the question, "How does the probability density per unit area of seeing one of these tracks become related to the square of the magnitude of the incident wave function?"

A spherical wave, emitted from a point source and impinging on a spherical scintillation screen centered on the source, will produce coherent packets all having the same values for $\int |\psi|^2 \, d^3x$. This is because the dimensions of the packets are determined by the sensitive medium. Because of the spherical symmetry of the screen, repeated identical waves arising at the screen will produce a uniform distribution of scintillations. The value of $|\psi|^2$ must also be uniform at this surface for the same reason. Thus, for this simple example, the proportionality of the probability distribution and $|\psi|^2$ certainly holds.

It is also true that $|\psi|^2$ decreases with the inverse square of the distance from the source. A comparison of the scintillation density on one spherical screen with that on another of a different radius shows that this density also decreases with the inverse square of the distance from the source because the scintillations are distributed over areas that increase with the square of the distance. Thus, again, the probability distribution is proportional to the magnitude squared of the wave function. If the screen has portions at different distances from the source, it is necessary to resort to a proof developed independently by Graham and Hartle [10]. A variant of this proof is presented in Appendix A.

The Stern-Gerlach measurement of a spin component has frequently been used as an example of the application of measurement theory. In Appendix B, this experiment is employed to illustrate some properties of wave functions that are used in this analysis of detectors.

II. TRACKS IN A CLOUD CHAMBER

Since we anticipate that α waves will look like particles in a cloud chamber, we begin by breaking the α wave into a superposition of small packets ψ_i as shown in Fig. 3. Each of these packets can then behave very much like a particle. These α wave packets remain relatively intact during the interaction with the cloud chamber (whose state is represented by χ) because the effect of each atom on a packet is quite small (except for a very few close approaches to atomic nuclei that we shall not consider). This is clear from the study of the passage of heavy particles through various media conducted by Bohr [8], Bethe and Ashkin [11], and others. This is why the wave function for a system composed of an α wave interacting with a cloud chamber can be written at some instant of time, to a good approximation, as the sum of products,

$$\Psi = \sum_i \psi_i \chi_0 + \sum_j \psi_j \chi_j \ . \tag{2.1}$$

The wave function Ψ is for a system composed of the α wave and the cloud chamber. The first sum (over i) is over terms involving the packets ψ_i that have not yet reached the cloud chamber, and the second one (over j) is over terms with packets ψ_j that have passed into the cloud chamber. The wave function χ_j includes the ionization track in some stage of formation by ψ_j as it moves along in the cloud chamber.

The packets in the first sum are coherent since all of the ψ_i's are multiplied by the same function χ_0 representing the undisturbed state of the cloud chamber. The χ_0 can be factored out and the packets combined to produce an incident plane wave ψ_0 so that the first sum reduces to $\psi_0 \chi_0$.

It is necessary to decide on the size of these packets. A minimum size is set by the uncertainty principle since a packet that is too small when it enters the sensitive medium will have large momentum components and will expand to too large a size before it comes to rest or departs from the chamber. One rather arbitrary way to define the size of a minimum packet is to choose a packet radius (at packet half maximum) as it enters the cloud chamber in the following way. See Fig. 4. By solving the Schrödinger equation, the dimensions of the packet can be determined after it has traveled some distance into the chamber. We can choose this distance to be from

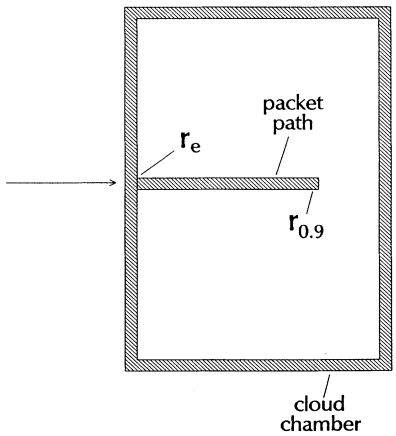

FIG. 4. The packets enter the cloud chamber and each forms a track. A minimum size of a packet is chosen by minimizing $(r_e^2 + r_{0.9}^2)^{1/2}$ where r_e is the radius of the packet when it enters the sensitive medium, and $r_{0.9}$ is its radius at 0.9 of the distance to the end of its path.

the place where it enters the cloud chamber either to the point where it leaves the medium, or to the point nine-tenths of the way to the end of the track. We choose the entering thickness to be the one that minimizes the sum of the squares of these two radii. This procedure produces packets whose sizes, while they are in the cloud chamber, are of the order of an α wave length. Any similar procedure would, of course, be satisfactory. For a 5 MeV α wave, the de Broglie wavelength is about 6.4×10^{-5} Å. Although this sets a minimum size to a packet, we shall see that portions of a number of them are coherent and can be combined to form larger packets whose sizes are determined by properties of the medium containing the ionization track.

The α wave can be expressed as a superposition of narrow bands parallel to the face of the cloud chamber, and each of these bands can be expanded in terms of these minimum packets just as it approaches the cloud chamber. See Fig. 3. The expansion can be written approximately in terms of Gaussians [12], or more precisely in terms of functions similar to the Wannier functions [13] of solid-state theory. Since the Schrödinger equation for the system is linear, it can be solved either backwards or forward for each term in Eq. (2.1) individually. The final wave function for the system at any time can then be reconstituted as a sum of the components produced by the wave packets.

An α packet, moving through the sensitive medium of the cloud chamber, will be accompanied by its electric field much like that of a charged particle. See Fig. 5. This electric field will sweep over neighboring atoms as the packet passes by [8]. This imparts impulses to the electrons in these atoms if vacant states are available to them. This will ionize some of the atoms and excite others. The electrons from the ionized atoms may then, in turn, ionize and excite other atoms until their energies are degraded below a critical value. In this way, each packet in the cloud chamber will be surrounded by excited atoms and ions for a small distance in the direction of its motion and to the sides with a long wake trailing out behind as shown in Fig. 6. Droplets condense on the ions to form a visible track whose width is the order of a tenth of a millimeter like those shown in Fig. 1.

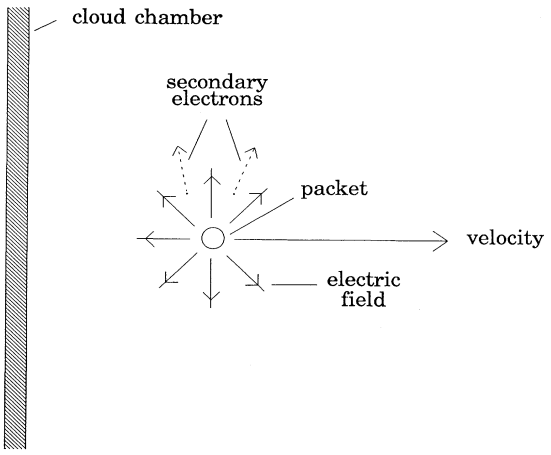

FIG. 5. As a packet moves through the cloud chamber, its electric field sweeps over the atoms, imparting an impulse to each electron. This excites some of the atoms and ionizes others.

The wave function of the cloud chamber χ_j can be approximated by a product of the wave functions of its atoms where χ_{ja} represents the wave function of the ath atom in the state associated with the jth packet. In addition, each atomic wave function can be written as the sum of an undisturbed (ground) state χ^0_{ja} and excited states χ^e_{ja}. Of course those atoms outside the wake will have a negligible excited component. In addition, the excited component for each atom will be small relative to its ground state because of the weakness of the electromagnetic interaction and the rapidity of the passage of a 5-MeV packet. Thus a cloud chamber wave function can be written approximately in the form

$$\begin{aligned}\chi_j &= \prod_a \chi_{ja} = \prod_a (\chi^0_{ja} + \chi^e_{ja}) \\ &\approx \prod_a \chi^0_{ja} + \sum_b \chi^e_{jb} \prod_{a\ (\neq b)} \chi^0_{ja} \\ &\approx \left(\prod_a \chi^0_{ja}\right)\left(1 + \sum_b \chi^e_{jb}/\chi^0_{jb}\right) . \end{aligned} \tag{2.2}$$

The atomic wave function for an atom χ_{ja} is a function of the coordinates of the atomic nucleus and electrons.

The wake w_j produced by the jth packet is composed of all of the excited states so that it is the excited part of the last expression, namely,

$$w_j = \prod_a \chi^0_{ja} \sum_b \chi^e_{jb}/\chi^0_{jb} . \tag{2.3}$$

Substituting this into Eq. (2.2) and that, in turn, into Eq. (2.1) then gives, at some instant of time, a wave function for the α-wave plus cloud-chamber system of

$$\Psi = \psi_0\chi_0 + \sum_j \psi_j(\chi^0_j + w_j), \tag{2.4}$$

where

$$\chi^0_j = \prod_a \chi^0_{ja} \tag{2.5}$$

is the undisturbed component of the cloud chamber wave function left by the jth packet.

FIG. 6. A wake w_j of excited and ionized atoms is produced by each packet ψ_j. Droplets condense on the ions to form a visible track.

The packets appearing in the last equation are of the minimum size allowed by the uncertainty principle. As we have noted, since the packets in the first term of Eq. (2.1) were all multiplied by the same factor, they could be combined to form the incident plane wave ψ_0. The question now arises whether the α packets in the second term on the right-hand side of Eq. (2.4) can be combined in a like manner. Since the atoms in the cloud chamber are excited in different ways by different packets, it appears that the wakes w_j (and, therefore, χ_j^0) will all be different. This suggests that the packets multiplying these wakes cannot be combined. However, this is not entirely true as we shall see.

In order to combine packets represented by ψ_j's multiplying w_j in Eq. (2.4), it is necessary to find w_j's that are identical. Although the w_j's are all different, we can find components of some of them that are the same as follows. Select one w_j and call it $w_{j'}$. Since the w_j's are wave functions involving the coordinates of the atoms of the cloud chamber, each w_j can be written as the sum of its $w_{j'}$ component and the remainder orthogonal to it. Thus,

$$w_j = a_{jj'} w_{j'} + \chi_{jj'}, \tag{2.6}$$

where $a_{jj'}$ is the scalar product of $w_{j'}$ and w_j, and $\chi_{jj'}$ is orthogonal to $w_{j'}$. This expression can be substituted into Eq. (2.4). Then all of the ψ_j's multiplying $w_{j'}$ can be combined to form the larger packet,

$$\psi'_{j'} = \sum_j \psi_j a_{jj'} \ . \tag{2.7}$$

See Fig. 7.

We have been employing an expansion of the α wave in terms of minimum packets ψ_j. It now appears possible to combine these minimum packets into the larger packets ψ'_j defined in Eq. (2.7) and shown in Fig. 8. The size of these larger coherent packets is considered in Appendix C. An approximate expansion of the α wave in terms of them can be obtained by the same procedure used above for minimum packets. Of course this new expansion will space these larger packets a greater distance apart. This expansion replaces Eq. (2.4) by

$$\Psi = \psi_0 \chi_0 + \sum_j \psi'_j \chi_j^{0\prime} + \sum_j \psi'_j w'_j, \tag{2.8}$$

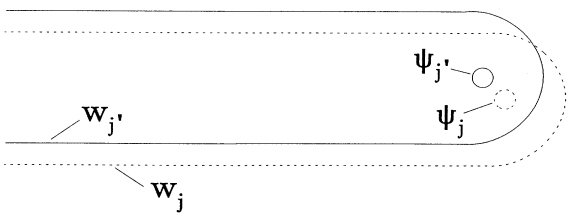

FIG. 7. The wake w_j of the packet ψ_j has a component $a_{jj'} w_{j'}$. This component multiplied by ψ_j can be combined with the term $\psi_{j'} w_{j'}$ to form $(\psi_{j'} + \psi_j a_{jj'}) w_{j'}$ in the wave function for the α-wave plus cloud chamber system.

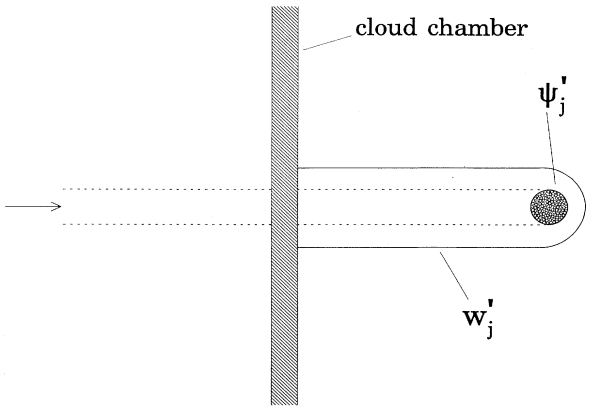

FIG. 8. Components of the minimum packets ψ_j can be combined with $\psi_{j'}$ in the manner shown in Fig. 7. This forms a larger packet $\psi'_{j'}$. The Schrödinger equation can be solved forwards and backwards in time to determine the path of this larger packet together with its disturbances of the medium.

where $\chi_j^{0\prime}$ is the undisturbed part of the cloud chamber wave function, and w'_j is the wake produced by the packet ψ'_j. The first term on the right-hand side represents that part of the wave function produced by packets that have not yet arrived at the cloud chamber, the second term is generated by the unscattered part of the α wave for packets in or past the cloud chamber, and the last term includes the scattered α waves and the concurrent excited atomic states (the wakes).

III. THE COLLAPSE TO ONE TRACK

It is clear from Appendix C that the mechanisms in the cloud chamber that produce the tracks of cloud droplets determine the size of the largest α packet ψ'_j that can be associated with a track. These packets, in some sense, replace the classical particles employed in the published explanations of these tracks. The last equation shows, however, that a large number of tracks are produced by the α wave from a single nuclear transition, one for each ψ'_j. Nevertheless, we see only a small number (see Fig. 1), actually, no more than one per nuclear transition. In order to understand what happens to all but one track produced by an α wave, it is necessary to include the observation mechanism (e.g., a camera) in the system. This entire system will be represented by a wave function that we shall call Ψ'.

The observer interacts with the cloud chamber by seeing the light from an outside source that it reflects. If no track is seen, the observer's state can be represented by ϕ_0. As before, because of the linearity of the equations, we solve the Schrödinger equation for the term in the wave function involving each packet individually as it generates its wake in the cloud chamber which finally interacts with the observer. Then we can combine the terms to form the wave function Ψ'. Since the observer interacts with the cloud chamber by seeing the droplets associated with each track, only the term in Eq. (2.8) con-

taining the wakes can interact with the observer's wave function. Each wake w'_j produces a state of the observer represented by a wave function ϕ_j having the record of a track. Each factor w'_j will be multiplied by a ϕ_j while the other terms are multiplied by ϕ_0. Thus the wave function for the whole system will take the form

$$\Psi' = \psi_0\chi_0\phi_0 + \sum_j \psi'_j\chi_j^{0\prime}\phi_0 + \sum_j \psi'_j w'_j\phi_j \qquad (3.1)$$

after observation.

Since this wave function can be constructed by following the effects of one packet at a time with the other packets not present, each ϕ_j represents the recording of only one track, the one generated by ψ'_j. Because of the linearity of the Schrödinger equation, there is no evidence available in the record represented by ϕ_j to indicate the existence of the other tracks. Thus the observer sees only one track for each α wave and is unaware of all the others. More than one track appears in Fig. 1 because a large number of *different* α waves are being emitted by many nuclei.

IV. THE PROBABILITY DISTRIBUTION

The above analysis can be applied to other devices that involve ionized wakes produced by electrons, photons, and other kinds of waves. For example, fluorescent screens were used by Rutherford [9] to detect α waves. He observed the scintillation on a screen created by the wake of excited atoms generated by each α wave packet ψ'_j penetrating the fluorescent materials. In a similar manner, a large number of electron waves produce scintillations on a screen that merge into a picture in an electron microscope. The densities in space of these scintillations and of tracks appearing in a cloud chamber are observed to be proportional to the square of the magnitudes of the incident waves. The explanation of this connection between the wave function and the probability distribution is as follows.

Consider the electron waves scattered from a bright point on an object being viewed in an electron microscope. See Fig. 9. Because it is a point, the waves scattered from the object will be emitted spherically symmetrically. They can impinge on a photographic plate that records the image. We shall select a photographic plate in the form of a complete sphere centered on the point object. The above analysis implies that the interaction of the electron waves with the plate will produce small packets ψ'_j that couple with wakes of excited atoms w'_j that remain in the "exposed" photograph. In the case of a single electron wave emitted by a single atom, a state of the plate ϕ_j is generated by the packet ψ'_j and contains no evidence of the other packets produced by the same atomic transition because of the linearity of the Schrödinger equation.

The first term on the right-hand side of Eq. (3.1) represents the part of the wave function that has not reached the sensitive medium as shown in Fig. 3. If we have an incident wave that has a finite radial extent, and we write

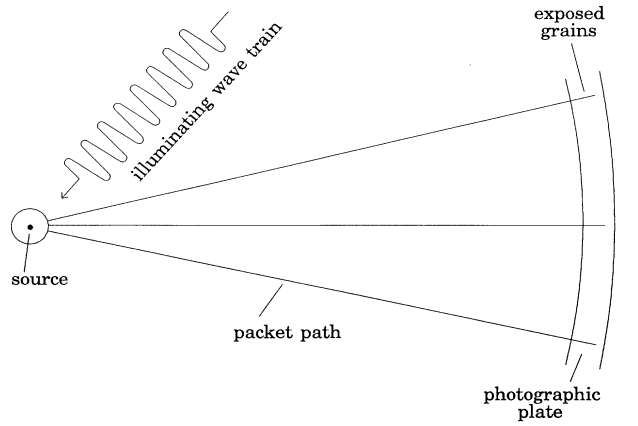

FIG. 9. The centers of electron packets ψ'_j generated in the photographic plate have followed straight paths from the point source.

the wave function after all of it has passed into the photosensitive medium and has stopped, the first term will vanish. If the medium absorbs all of the incident wave, none of the unscattered α wave will remain, and the second term in Eq. (3.1) will not appear. In this case, we can label each component of the last term with the coordinates of the point on the inner surface of the medium and the time of entrance x of the center of the packet and write the wave function as

$$\Psi' = \sum_x \psi'_x w'_x \phi_x, \qquad (4.1)$$

where we have used a discrete set of x's.

This is the wave function for the system after one electron wave has come to rest in the photographic plate. If a second identical electron wave is emitted from the source, it will find the system in the state represented by the above wave function and will finally produce

$$\Psi^{(2)\prime} = \sum_{x^2}\sum_{x^1} \psi^{(2)\prime}_{x^2}\psi^{(1)\prime}_{x^1} w^{(2)\prime}_{x^2} w^{(1)\prime}_{x^1} \phi_{x^2x^1} \qquad (4.2)$$

where the superscripts on the right-hand side indicate which of the two electrons is represented. Each $\phi_{x^2x^1}$ represents a state of the photographic plate with two strings of exposed grains.

After a large number n of these electron wave functions have reached the plate, the wave function of the system will have the form

$$\Psi^{(n)\prime} = \sum_{x^n}\cdots\sum_{x^2}\sum_{x^1} \psi^{(n)\prime}_{x^n}\cdots\psi^{(2)\prime}_{x^2}\psi^{(1)\prime}_{x^1} w^{(n)\prime}_{x^n} \times\cdots w^{(2)\prime}_{x^2} w^{(1)\prime}_{x^1} \phi_{x^n\ldots x^2x^1} . \qquad (4.3)$$

Each sequence of coordinates appearing as the subscript of $\phi_{x^n\ldots x^2x^1}$ locates the positions of strings of exposed grains recorded in a state of the photographic plate. They are the sequences that would result if the string coordinates for each state were drawn at random from an ensemble where the coordinates of each string are assigned

equal probability. Since the plate is spherically symmetric with respect to the scattering center, the strings must be uniformly distributed over its surface so that the probability distribution is uniform. Since the photographic material interacting with each packet is the same, each packet has an equal volume. The spherical symmetry guarantees that the amplitude of the incident α wave at the plate is uniform over the surface. Thus the value of $\int |\psi|^2 \, d^3x$ for all the packets is the same. As a result the probability distribution of a string of exposed grains occurring at x is proportional to $\int |\psi|^2 \, dt$ where the integration is over the time required for the wave to pass into the plate.

If we make the same measurements with a second piece of apparatus differing only in the distance from the scattering center to the plate, the probability distributions for the two cases must be spread evenly over the two spherical plates and have magnitudes in inverse proportion to their areas or inverse proportion to the square of their distances from the source. Since the magnitude squared of the wave amplitude must also fall off as the inverse square of the distance, the probability distribution per unit area must be proportional to the magnitude squared of the wave amplitude in these cases.

If a magnetic lens is placed in the path of the electron waves, they can be focused to the vicinity of some point on the photographic plate as shown in Fig. 10. If the Schrödinger equation is solved backwards in time, the packets and wakes formed in the plate will be diverging as we proceed backwards toward the source. The centers of the packets will diverge out of the surface of the plate and proceed along curved paths to form a uniform spherical distribution near the point scatterer. When no lens is present as in Fig. 9, the volume of the packets ψ_j' will be determined by the medium through which they proceed in the photographic plate. When the lens *is* present, the packets at the plate will be moving in the same medium but along paths at different angles with the surface. Since it is the bulk properties of the medium that determine the volumes of the packets, the packets will all have the same volume. Since their distances from the scattering source is essentially the same, they will each carry the same quantity of $\int |\psi|^2 \, d^3x$. Thus the density of packets entering the surface of the sensitive medium will be proportional to $|\psi|^2$ and is, of course, proportional to the probability of recording a string.

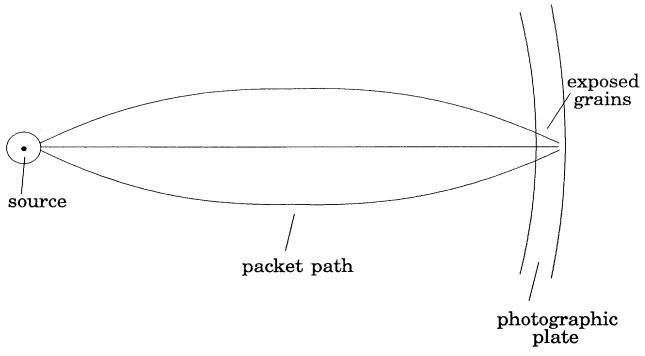

FIG. 10. A lens will bend packet paths that diverge radially from the source so that they almost focus on a point. Since each packet has the same volume at the plate and has traveled approximately the same distance from the source, it will have the same value of $\int |\psi|^2 d^3x$ as any other.

The cases that we have just considered have been easy to analyze because each packet has the same value of $\int |\psi|^2 \, d^3x$. In general, the considerations are more complicated. Graham and Hartle [10] have made the more general analysis possible by determining the dependence of the wave function in Eq. (4.3) on the frequency of occurrence of a given value x as the number n of identical electron states ψ_x increases to a large value. A variant of their derivation is found in Appendix A. If the w_x's and the ϕ are normalized to unity, they find that the magnitude squared of the wave function can be expressed in the form

$$\langle \Psi' | \Psi' \rangle \sim \int_0^1 \delta(f_x - |\psi(x)|^2) \, df_x \ , \tag{4.4}$$

where f_x is the number of times that x occurs in a term in Eq. (4.3), divided by n. It is clear from this result that only those terms in Eq. (4.3) that have the frequency of occurrence of any particular value of x infinitesimally close to $|\psi(x)|^2$ will contribute appreciably to Ψ' in this limit. This is equivalent to saying that the distribution of the frequencies of occurrence of scintillations at x is a δ function centered on $|\psi(x)|^2$. This is, of course, equivalent to the probability distribution of the occurrence of a scintillation at x if one wave function ψ strikes the scintillation screen.

V. DISCUSSION

In Sec. II, it was noted that a wave incident on the sensitive medium of a detector can be written as a superposition of coherent packets ψ_j', each of which is associated with a state of the observer. By solving the Schrödinger equation backwards, the previous course of each of these packets, whose size is determined by the detector, can be determined. These are the packets that are essential for the explanation of the "quantum jumps" in the intensity of laser light scattered off of a single trapped atom [3]. In those experiments, the scattered light was detected by a photomultiplier tube. In that case, this light penetrated the plate of the photomultiplier and excited atoms, some of whose electrons left the plate. The wavelength of the incident light was large compared to the interatomic spacing so that the minimum packets ψ_j that we would form would extend over many atoms. The electrons leaving the ionized atoms had relatively little energy so that they could not be expected to ionize many additional atoms. Thus the packets of light ψ_j' could not have been much larger than the minimum packets formed in the photomultiplier plate, that is, much larger than the wavelength of the incident light.

The problem of explaining how waves can have the appearance of classical particles has been studied for many years by many researchers with a number of approaches. Two recent review articles on this subject have been writ-

ten by Omnès [14] and by Schulman [15] and contain references to a number of papers.

Green [16] has considered the effect of the interaction of a system with an environment made up of harmonic oscillators. He finds that off-diagonal elements of the density matrix of the system in the proper representation are destroyed by the interaction with the environment. This is necessary if the system is to have the appearance of a classical one. However, his conclusions are contested by Furry [17]. Zurek [18] and others have also found that the off-diagonal elements disappear as a result of decoherence as a consequence of the interaction with the environment. A brief summary is presented in a Letter by Zeh [19]. This effect of the environment on the density matrix of a system is similar to the finding made here that the environment composed of the sensitive medium of a detector, by forming coherent packets, causes an incident wave to appear like a particle. Gell-Mann and Hartle [20] have studied the conditions under which histories can be identified as having decohered, especially for use in cosmology.

This work suggests that the particle concept is unnecessary in quantum mechanics since particlelike phenomena appear to be explainable in terms of waves (fields). This is in line with Everett's [21] proposal that there is no need for a "collapse of the wave function" and that the universe is represented by a single super wave function. It, therefore, eliminates a number of the paradoxes that appear in the standard interpretation of quantum mechanics such as, for example, "Schrödinger's cat" [22].

Still, physicists have been trained in the wave-particle concept and may resist strongly giving it up. They may ask if the particle analysis is not equivalent to the above wave explanation of ionization tracks. Are there any experimental differences in the predictions of the two theories? There should be a difference in the density of the inner parts of a track in a cloud chamber or a photographic plate since wave mechanics calls for a packet of some extent which would be approximated by an extended charge. The particle concept calls for a point charge. Thus the electric fields originating from the detected entity would be different near the center of a track in the two cases. The strong field near a particle should produce a more dense track in its vicinity than that produced by a packet.

If, indeed, there is no need for the particle concept in quantum mechanics, then the universe must be constructed entirely of fields. Fundamental entities such as electrons become identified with fields or waves.

ACKNOWLEDGMENTS

The author is indebted to the following colleagues at the University of Florida for reading the manuscript and making suggestions: R. L. Coldwell, H. P. Hanson, J. R. Klauder, H. J. Monkhorst, S. Detweiler, and F. E. Dunnam. In addition, H. S. Green, L. S. Schulman, and Andrei Lindei have been kind enough to discuss this problem.

APPENDIX A: FREQUENCY DISTRIBUTION FOR LARGE n

Graham and Hartle [10] have found the magnitude of the wave function in Eq. (4.3) in the limit of large n in terms of the frequency of occurrence of a particular value x. Their analysis is similar to the following.

If the w's and ϕ's in Eq. (4.3) are normalized to unity, then the magnitude of the amplitude squared is given by

$$\langle\Psi'|\Psi'\rangle = \sum_{x^1\cdots x^n} \langle x^1|x^1\rangle\langle x^2|x^2\rangle\cdots\langle x^n|x^n\rangle, \tag{A1}$$

where $\langle x^i|x^i\rangle$ is the magnitude squared of ψ_{x^i}. The terms in the sums on the right-hand side of the last equation can be sorted according to the number of times j that a scalar product with a particular value x occurs, that is, according to the number of scintillations that occur in the infinitesimal area at x. The result is

$$\langle\Psi'|\Psi'\rangle = \sum_{j=0}^{n} T_j = 1, \tag{A2}$$

where

$$T_j = \binom{n}{j}\langle x|x\rangle^j \sum_{x^1\cdots x^{n-j}}{}' \langle x^1|x^1\rangle\cdots\langle x^{n-j}|x^{n-j}\rangle\ , \tag{A3}$$

and the prime on the sum indicates that x is excluded.

Since

$$\sum_{x^\ell}\langle x^\ell|x^\ell\rangle = 1\ , \tag{A4}$$

we can write

$$\begin{aligned} T_j &= \binom{n}{j}\langle x|x\rangle^j \prod_{\ell=1}^{n-j}\left(\sum_{x^\ell}{}'\langle x^\ell|x^\ell\rangle\right) \\ &= \binom{n}{j}\langle x|x\rangle^j(1-\langle x|x\rangle)^{n-j}\ . \end{aligned} \tag{A5}$$

The series in Eq. (A2) has most of its contributions concentrated around a maximum term (labeled by j_m) in the limit as n increases. This allows us to approximate the terms using Stirling's approximation which gives

$$\binom{n}{j} \sim \frac{n^{n+\frac{1}{2}}}{j^{j+\frac{1}{2}}(n-j)^{n-j+\frac{1}{2}}\sqrt{2\pi}}\ . \tag{A6}$$

This can be substituted into Eq. (A5) and the logarithm taken. Differentiating the result with respect to j and setting it to zero gives an expression solved by

$$j_m = n\langle x|x\rangle \tag{A7}$$

for the value of j that maximizes T_j. Differentiating ln T_j twice and substituting this value of j_m gives

$$\frac{d^2\ln T_j}{dj^2} \sim -[n\langle x|x\rangle(1-\langle x|x\rangle)]^{-1} \tag{A8}$$

at the maximum term. These expressions allow us to

expand ln T_j around the maximum to second order in j and to obtain

$$T_j \sim (2\pi n\langle x|x\rangle)^{-1/2} e^{-(j-n\langle x|x\rangle)^2/(2n\langle x|x\rangle(1-\langle x|x\rangle))} . \tag{A9}$$

Instead of the number of times j that a scalar product with x appears in a term in Eq. (A1), we can use the *frequency* of occurrence of x, namely,

$$f_x = j/n . \tag{A10}$$

Then, according to Eq. (A7), the maximum value of T_j occurs at f_x equal to $\langle x|x\rangle$. The expression in Eq. (A9) is such that the limit of nT_j as n increases is a δ function. As a result,

$$\langle \Psi'|\Psi'\rangle \sim \int_0^1 \delta(f_x - \langle x|x\rangle)\, df_x . \tag{A11}$$

This shows the limiting frequency distribution for the occurrence of x in the terms in Eq. (A1).

APPENDIX B: A STERN-GERLACH EXAMPLE

Consider the use of a Stern-Gerlach (SG) device to measure the spin component of a neutral packet with a large total spin oriented perpendicular to the axis of the magnetic field as shown in Fig. 11. The packet is collimated by a slit, and then an inhomogeneous magnetic field splits it into subpackets, each corresponding to a spin component. (The coils are omitted for the moment.) The paths of these packets are finally focused so that they pass through a common intersection region marked A. If the magnetic lens system is designed to pass this combined packet from region A through a second SG device rotated to the direction of the spin of ψ_i, the spin component will be shown to be the same as the initial packet. This demonstrates that the subpackets were "coherent" when they reached region A.

As noted in Ref. [3], the form of the wave function at any time during its passage through the apparatus can be determined by first finding the course of each subpacket by solving the Schrödinger equation forward or backwards in time. Since the equation is linear, the solution for the entire wave function is given by the sum of all of the packets at the desired time.

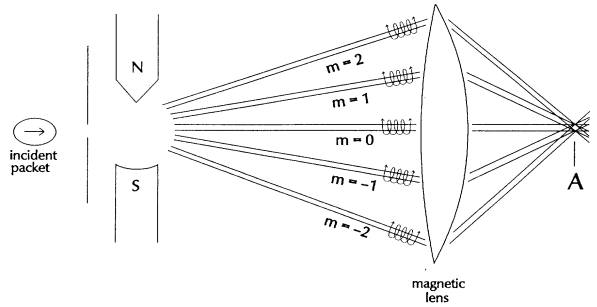

FIG. 11. A Stern-Gerlach experiment to measure the spin component of a packet and a magnetic lens that converges all subpackets to overlap in region A. The coils are connected to recorders.

The initial wave function of the first SG device (shown in Fig. 11) plus the packet will have the form

$$\Psi_i = \psi_i \chi_i , \tag{B1}$$

where Ψ_i is the initial wave function for the system composed of the SG device and the packet. The state of the initial packet alone is represented by ψ_i while the initial state of the SG device is χ_i. In terms of the wave functions of the individual subpackets, the wave function looks like

$$\Psi_s = \chi_i \sum_m \psi_m , \tag{B2}$$

where m represents the spin component of the subpacket. The SG device returns to its initial state when the packets have passed on. When the subpackets have merged again in region A, the wave function is finally

$$\Psi_f = \psi_A \chi_i , \tag{B3}$$

where

$$\psi_A = \sum_m \psi_m . \tag{B4}$$

This is, of course, a spin function with the spin oriented in the same direction as in ψ_i. The fact that the apparatus returns to its initial state χ_i allows the addition of the component packets ψ_m just as this fact allows for the coherent scattering of visible light passing through a cloud chamber.

On the other hand, we can arrange to measure the spin component by placing a coil around each path followed by a subpacket (as shown) and connecting each coil to a different amplifying and recording device (not shown). The dipole magnetic moments of the packets induce currents in the coils that are amplified and recorded. In this case, χ represents the state of the SG device together with the recorders. In the initial state χ_i, the recorders have registered no signals and the wave function is that in Eq. (B1). Similarly, Eq. (B2) represents the wave function before the subpackets have reached the coils.

Now, however, in the wave function after the subpackets have reached the path intersection region A of Fig. 11, the packets cannot be combined as they were in Eq. (B3). To see this, we solve the Schrödinger equation for the system with each subpacket separately and derive the final wave function by adding the final wave functions together. The result is

$$\Psi_f = \sum_m \psi_m \chi_m , \tag{B5}$$

where χ_m is the state of the SG device, the amplifiers, and the recorders when the subpacket ψ_m has passed through. These states χ_m are orthogonal to each other since they represent the rearrangement of entirely differ-

ent atoms in the recorders into new states. This prevents the summation of the wave functions ψ_m with a χ_i factored out as was done in Eq. (B3), and we say that the ψ_m's are "incoherent." This inability to add the ψ_m's into a single wave function in region A of Fig. 11 means that a measurement of the spin component in that region by an SG device oriented along the direction of the initial packet will not show a single spin component as it did before the coils were included in the apparatus. Each subpacket will remain with its spin orientation. This shows that the subpackets are "incoherent" in region A. The sensitive medium in a cloud chamber behaves like the coils and attached recorders in preventing the separate tracks associated with pieces of the α wave from being merged into a continuous clouded region.

Suppose now that an observer, whose wave function is represented by ϕ, looks at the recorders to see what spin component has been indicated by the meters on their fronts. As before, we can determine the final state of the entire system including the observer by following, with the aid of the Schrödinger equation, each one of the subpackets as it moves through the system producing the final interaction with the observer. Then we can add these wave functions together to form the entire wave function. The final wave function will then have the form

$$\Psi_f = \sum_m \psi_m \chi_m \phi_m \ , \tag{B6}$$

where ϕ_m represents the state of the observer that involves a memory of the reading of one measurement result, namely, m. This is why the observer sees only one meter reading its spin component, and, for similar reasons, he sees only one track in a cloud chamber.

Now it could be true that the apparatus is not as powerful as the one pictured in Fig. 11, that is, it can determine only if the spin component lies within a range of values rather than its specific value. This would be the case if a single coil were wrapped around several packet paths rather than just one as shown. We label each coil by a value of r. Then Eq. (B5) would be replaced by

$$\Psi_f = \sum_r \sum_m^r \psi_m \chi_r, \tag{B7}$$

where $\sum_m^r$ represents the sum over the values of m in the range r, and χ_r indicates a state where a recorder has indicated a registered signal in the range r.

If the observer is watching the meter indicating these ranges, the final state of the system including the observer is given by

$$\Psi'_f = \sum_r \sum_m^r \psi_m \chi_r \phi_r, \tag{B8}$$

where ϕ_r indicates a state of the observer with the memory of a meter reading in the range r. This corresponds to a cloud chamber being seen through defocused eyes.

If the observer wants a more precise measurement of the spin component of the packet, he can use an apparatus that will make finer distinctions by using coils that are wrapped around smaller numbers of subpacket paths. There is, however, an ultimate measurement using apparatus with coils around single paths as shown in Fig. 11. Any further refinement yields no more detail to the spin component structure. This is analogous to the observer of a cloud chamber who improves the focus of his eyes. If this is not sufficient to bring the image of the track down to its ultimates size, magnifying lenses can be used to diminish the image to its minimum size. We are accustomed to assigning this minimum size to the true dimensions of the track.

APPENDIX C: PACKET DIMENSIONS

Equation (2.7) shows how a coherent packet ψ'_j can be constructed from minimum packets. The dimensions of this packet depend upon the distances apart of the jth and j'th packets for which $a_{jj'}$ is significant, that is, where the scalar product of two wakes produced by minimum packets is not negligible. This, in turn, depends upon the scalar products of the excited wave functions of the atoms composing the sensitive medium in the respective wakes. From the form of the wave function for the wake in Eq. (2.3),

$$\begin{aligned} a_{jj'} &= \sum_b \prod_{a\ (\neq b)} (\chi^0_{ja}|\chi^0_{j'a})(\chi^e_{jb}|\chi^e_{j'b}) \\ &= \prod_a (\chi^0_{ja}|\chi^0_{j'a}) \sum_b \frac{(\chi^e_{jb}|\chi^e_{j'b})}{(\chi^0_{jb}|\chi^0_{j'b})}, \end{aligned} \tag{C1}$$

where $(\chi^e_{jb}|\chi^e_{j'b})$ is the scalar product of the excited portion of the wave function of the bth atom in the jth wake and the excited portion of the same atom in the j'th wake.

The ranges of $a_{jj'}$ in various directions relative to the direction of packet propagation is determined by the magnitudes of the excited portions of the atomic wave functions. In Fig. 12 is sketched a plot of the ratios of the squares of the magnitudes of the excited portions to the square of the magnitudes of the unexcited portions

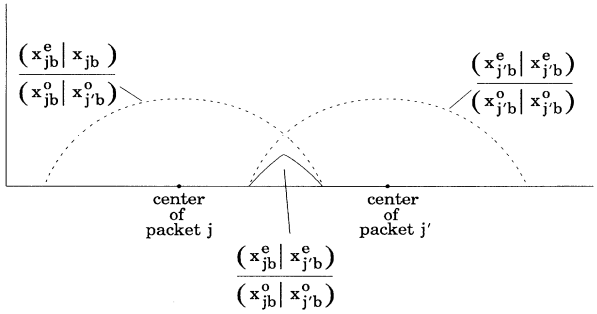

FIG. 12. Plots of the ratios of scalar products of atomic wave functions for atoms along a line perpendicular to the directions of packet motion to indicate the wakes of packets labeled j and j' and the extent of contributions to $a_{jj'}$ as b is summed over these atoms in Eq. (C1).

for the atoms along a line perpendicular to the direction of packet propagation passing through the centers of the minimum packets labeled j and j'. The magnitudes of the unexcited components are almost unity because of the smallness of the scattered waves. These sketches indicate the forms for the wakes of the two minimum packets. The scalar products between these states $(\chi^e_{jb}|\chi^e_{j'b})/(\chi^0_{jb}|\chi^0_{j'b})$ are also shown by the solid line. This last ratio must vanish when the magnitudes of the excited states vanish. As a result, the solid line is on the horizontal axis when either of the other two (dashed) curves is on that axis.

As we have previously noted, the wake for a minimum packet has a transverse half-width equal to the maximum distance from the packet for which the energies imparted to the atomic electrons is sufficient to ionize the atoms. It is clear from the last equation, and from the figure, that $a_{jj'}$ will become small when the distance between the two packets exceeds twice this half-width, that is, twice the electron ionization range. Thus the transverse half-width of ψ'_j is, according to Eq. (2.7), equal to twice the electron ionization range. Since the large packet ionizes atoms out beyond its boundary a distance equal to the electron ionization length, the half-width of the visible track should be of the order of four times the electron ionization range.

Ahead of a minimum packet progressing through the medium, atoms will be excited in much the same manner as for the transverse directions. Behind the packets, the atomic states will decay and the molecules of the medium will change positions with time. Thus the extent of the $a_{jj'}$'s ahead of and behind the packet must also depend upon the medium.

When these larger packets are used to expand the incident wave, their spacing will be some fixed multiple of the electron ionization range. This is, of course, determined by the sensitive medium and is independent of the amplitude of the incident wave. The above analysis is roughly correct for α particles with energies of 5 MeV or greater. For energies sufficiently low for α particles and electrons, the incident packet will not follow a straight path in the medium and may even break up.

[1] N. F. Mott, Proc. R. Soc. London, Ser. A **126**, 79 (1929).

[2] W. Heisenberg, *The Physical Principles of the Quantum Theory* (Dover, New York, 1930).

[3] A. A. Broyles, Phys. Rev. A **45**, 4925 (1992).

[4] W. Heitler, *The Quantum Theory of Radiation*, 3rd ed. (Oxford University Press, New York, 1954). See pp. 193–194.

[5] G. Gamow, Z. Phys. **52**, 510 (1928); **51**, 204 (1928); R. W. Gurney and E. U. Condon, Nature (London) **122**, 439 (1928).

[6] J. von Neumann, *Mathematical Foundations of Quantum Mechanics* (Princeton University Press, Princeton, NJ, 1955).

[7] F. London and E. Bauer, in *Quantum Theory and Measurement*, edited by J. A. Wheeler and W. H. Zurek, (Princeton University Press, Princeton, 1955); E. P. Wigner, Am. J. Phys. **31**, 6 (1963).

[8] D. Bohr, K. Dan. Vidensk. Selsk. Mat. Fys. Medd. **XVIII**, No. 8 (1948); J. D. Jackson, *Classical Electrodynamics*, 2nd ed. (Wiley, New York, 1975), Chap. 13.

[9] E. Rutherford, Philos. Mag. **21**, 669 (1911).

[10] J. B. Hartle, Am. J. Phys. **36**, 704 (1958); Neill Graham and B. S. DeWitt, in *The Many-Worlds Interpretation of Quantum Mechanics*, edited by B. S. De Witt and Neill Graham (Princeton University Press, Princeton, NJ, 1973); B. S. DeWitt, Phys. Today **23** (No. 9), 30 (1970).

[11] H. A. Bethe and J. Ashkin, in *Experimental Nuclear Physics*, edited by E. Segré (Wiley, New York, 1953), Vol. 1, p. 166.

[12] Kodi Husimi, Proc. Phys. Math. Soc. Jpn. **22**, 264 (1940); see also p. 277. Husimi discusses von Neumann's approximate expansion in terms of Gaussians.

[13] G. Wannier, Phys. Rev. **52**, 191 (1937).

[14] Roland Omnès, Rev. Mod. Phys. **64**, 339 (1992).

[15] L. S. Schulman, Ann. Phys. (N.Y.) **212**, 315 (1991).

[16] H. S. Green, Nuovo Cimento **19**, 880 (1958).

[17] W. H. Furry, in *Boulder Lectures in Theoretical Physics*, edited by W. E. Brittin (University of Colorado Press, Boulder, 1966).

[18] W. H. Zurek, Phys. Rev. D **24**, 1516 (1981); **26**, 1862 (1982); Phys. Today **44** (No. 10), 36 (1991).

[19] H. D. Zeh, Phys. Lett. A **172**, 189 (1993).

[20] M. Gell-Mann and J. B. Hartle, in *Proceedings of the 3rd International Symposium, Foundations of Quantum Mechanics in the Light of New Technology*, edited by S. Kobayasahi, H. Ezawa, Y. Murayama, and S. Nomura (Physical Society of Japan, Tokyo, 1990); in *Complexity, Entropy and the Physics of Information*, edited by W. Zurek, Santa Fe Institute Studies in the Science of Complexity, No. 8 (Addison-Wesley, Redwood City, CA, 1991); J. J. Halliwell and J. B. Hartle, Phys. Rev. D 43, 1170 (1991).

[21] Hugh Everett II, Rev. Mod. Phys. **29**, 454 (1957), reprinted in *The Many-Worlds Interpretation of Quantum Mechanics*, edited by B. S. De Witt and Neill Graham (Princeton University Press, Princeton, NJ, 1973); in *Quantum Theory and Measurement*, edited by J. A. Wheeler and W. H. Zurek (Princeton University Press, Princeton, NJ, 1983).

[22] E. Schrödinger, Naturwissenschaften **23**, 807 (1935); **23**, 823 (1935); **23**, 844 (1935); translation by J. D. Trimmer, in *Quantum Theory and Measurement*, edited by J. A. Wheeler and W. H. Zurek (Princeton University Press, Princeton, NJ, 1983).

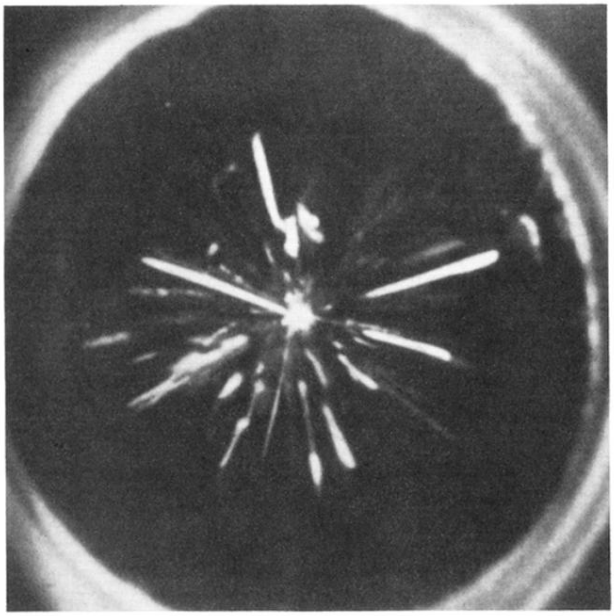

FIG. 1. Photograph of α tracks in a cloud chamber from a radioactive source in the center. The tracks do not cover the sensitive area of the cloud chamber although the wave function does. This is Fig. 41-44 from *Physics Demonstration Experiments*, edited by H. F. Meiners,